IOP Publishing Journal of Physics: Condensed Matter
J. Phys.: Condens. Matter **29** (2017) 205501 (6pp) https://doi.org/10.1088/1361-648X/aa693f

Diffusivity of the double negatively charged mono-vacancy in silicon

Chidanand Bhoodoo, Lasse Vines, Edouard Monakhov and Bengt Gunnar Svensson

Department of Physics, University of Oslo, Center for Materials Science and Nanotechnology, PO Box 1048 Blindern, N-0316 Oslo, Norway

E-mail: chidanand.bhoodoo@fys.uio.no

Received 10 February 2017, revised 13 March 2017
Accepted for publication 27 March 2017
Published 10 April 2017

Abstract

Lightly-doped silicon (Si) samples of *n*-type conductivity have been irradiated with 2.0 MeV H^+ ions at a temperature of 30 K and characterized *in situ* by deep level transient spectroscopy (DLTS) measurements using an on-line setup. Migration of the Si mono-vacancy in its double negative charge state (V^{2-}) starts to occur at temperatures above ~70 K and is monitored via trapping of V^{2-} by interstitial oxygen impurity atoms (O_i), leading to the growth of the prominent vacancy-oxygen (VO) center. The VO center gives rise to an acceptor level located at ~0.17 eV below the conduction band edge (E_c) and is readily detected by DLTS measurements. Post-irradiation isothermal anneals at temperatures in the range of 70 to 90 K reveal first-order kinetics for the reaction $V^{2-} + O_i \rightarrow VO\ (+2e^-)$ in both Czochralski-grown and Float-zone samples subjected to low fluences of H^+ ions, i.e. the irradiation-induced V concentration is dilute ($\lesssim 10^{13}$ cm^{-3}). On the basis of these kinetics data and the content of O_i, the diffusivity of V^{2-} can be determined quantitatively and is found to exhibit an activation energy for migration of ~0.18 eV with a pre-exponential factor of $\sim 4 \times 10^{-3}$ cm^2 s^{-1}. The latter value evidences a simple jump process without any entropy effects for the motion of V^{2-}. No deep level in the bandgap to be associated with V^{2-} is observed but the results suggest that the level is situated deeper than ~0.19 eV below E_c, corroborating results reported previously in the literature.

Keywords: mono-vacancy, silicon, thermal migration, DLTS, ion implantation, diffusivity

(Some figures may appear in colour only in the online journal)

1. Introduction

The mono-vacancy (V) in crystalline silicon (Si) is together with its self-interstitial counterpart (I) the most fundamental building block for high-order defects of zero, one, two and three dimensions in Si. Furthermore, both V and I can promote the diffusion of dopants and impurities, and thus influence the electrical, mechanical and optical properties of Si wafers even on macroscale. Spectroscopic identification of V has primarily been made via the pioneering work by Watkins and co-workers in the 1960s to 1980s using electron paramagnetic resonance (EPR) as the main characterization technique [1–6]. In contrast, no unambiguous spectroscopic signal of I has been detected experimentally and its existence is verified indirectly by trapping at impurities like aluminum, boron, carbon and oxygen [1, 2]. A major reason for the elusive nature of I is its high mobility even at liquid helium temperature (~4 K) during irradiation with MeV electrons [1], which is a commonly utilized method to enhance the concentration of isolated point defects in semiconductors.

The configuration and electronic structure of V are surprisingly well described by a straight-forward model where the electron states arise from highly localized molecular orbitals given by linear combinations of the broken bond orbitals of the four Si atoms surrounding V [2, 4]. The validity of this one-electron approach implies that electron–electron interaction is weak and crystal field effects prevail, decoupling the electrons. This was challenging to theorists and a long

standing controversy before being resolved by Lannoo, Baraff and co-workers [7, 8]. In its undistorted configuration, V exhibits tetragonal T_d symmetry with a set of singlet and triplet states. The singlet is lowest in energy (fully bonding) and accommodates two electrons with paired spins leading to a double positive charge state (V^{2+}), if the triplet state remains empty. A third electron will occupy the triplet state, which is degenerate and a tetragonal Jahn–Teller distortion takes place splitting the state. This lowers the total energy of the resulting single positively charged V^+ and the symmetry is reduced to D_{2d} with the unpaired electron equally distributed over the four surrounding Si atoms. A fourth electron, yielding V^0, will pair with the third electron and further increase the tetragonal distortion because of the energy gain of one more electron. A fifth electron occupies a higher split state of the original degenerate triplet one and V^- exhibits additional Jahn–Teller distortion and C_{2v} symmetry. The fifth electron resides primarily on 'one side' of V^- in a bond between a pair of the four Si atoms which distends slightly while the other pair pulls further together. A sixth electron, yielding V^{2-}, will possibly pair with the fifth electron but this lacks experimental evidence.

As follows from the description above, V can appear in at least five different charge states (2+, +, 0, −, 2−) where V^+ and V^- are paramagnetic and directly detectable by EPR [1–6]. From the EPR studies utilizing p-type and n-type materials of different resistivity, stress-induced alignment, and photo-excitation with different wavelengths, also indirect evidence for the existence of V^{2+}, V^0 and V^{2-} has been obtained. Because of the large Jahn–Teller distortions involved, the energy positions of the V charge state transitions cannot be accounted for by only considering the rising in the bandgap due to Coulomb repulsion between the added electrons, the so-called Hubbard correlation energy [9]. In particular, the gain in Jahn–Teller energy for the $V^0 \rightarrow V^+$ transition is high enough to overcome the Coulomb repulsion between the electrons such that the ionization energy of $V^0 \rightarrow V^+ + e^-$ exceeds that of $V^+ \rightarrow V^{2+} + e^-$ (e^- denotes an electron). That is, the energy level ordering is inverted and V is a negative-U defect, first predicted theoretically by Baraff *et al* [10] and later confirmed experimentally [11, 12]. The single donor level ($V^{+/0}$), is situated ∼0.03 eV above the valence band maximum (E_v) and the double donor ($V^{2+/+}$) ∼0.1 eV deeper at $\sim E_v + 0.13$ eV [5, 6]. Much less is known about the positions of the single and double acceptor states ($V^{0/-}$ and $V^{-/2-}$); however, they appear to be deeper than 0.17 eV below the conduction band minimum (E_c) since no levels shallower than that can be associated with V according to the deep level transient spectroscopy (DLTS) study by Troxell and Watkins [13]. This conclusion is also corroborated by the results in the present study.

The activation energy for thermal migration of V hinges strongly on the charge state with values of ∼0.45 eV and ∼0.32 eV for V^0 and V^{2+}, respectively, as revealed by EPR and DLTS measurements [3]. For V^{2-}, which prevails in n-type material, EPR data give a migration barrier of ∼0.18 eV [2], i.e. substantially lower than that for V^0 and V^{2+}. Corresponding DLTS data for V^{2-} are scarce in the literature and this is the main issue addressed in the present work studying a dilute concentration regime. The experimental concept used is based on trapping of migrating V^{2-} at interstitial oxygen atoms (O_i). Oxygen is the dominant residual impurity in Czochralski (Cz) grown silicon material with [O_i] typically in the 10^{17} cm^{-3} range (square brackets denote concentration). Also in float-zone (Fz) material, O_i is a major impurity with a typical concentration in the $10^{15} - 10^{16}$ cm^{-3} range. After V trapping by O_i, substitutional oxygen forms, commonly known as the VO center (or A center) [14–17]. The VO center is perhaps the most studied and abundant point defect in silicon irradiated/implanted at room temperature (RT), and it has been characterized by a wealth of optical, magneto-resonance, and electrical spectroscopic techniques. In contrast to O_i, VO is electrically active and gives rise to a characteristic single acceptor level at $\sim E_c - 0.17$ eV [15, 16], readily observed by DLTS in n-type samples. Hence, by performing *in situ* DLTS analysis after irradiation at cryogenic temperatures, where V^{2-} remains essentially immobile, the growth in [VO] during subsequent thermal treatment (annealing) can be monitored via the $E_c - 0.17$ eV level. The temperature dependence of the growth rate of [VO] is given by the activation energy for migration of V^{2-}($E_{\text{migr}}^{V^{2-}}$) and furthermore, if [O_i] is known also the pre-exponential factor of the V^{2-} diffusivity ($D_0^{V^{2-}}$) can be deduced.

Using lightly doped n-type Cz and Fz samples irradiated with MeV protons at cryogenic temperature, we obtain $E_{\text{migr}}^{V^{2-}} = 0.18$ eV, i.e. identical to the EPR-value reported by Watkins [2] studying counter-doped n-type Cz samples. Further, our value extracted for $D_0^{V^{2-}}$ suggests a simple jump process with no entropy effects for the V^{2-} migration. Finally, dynamic annealing is found to be strong even at cryogenic temperatures and the fraction of V's surviving recombination with I's is only on the order of 1%, similar to that found for irradiation/implantation at RT.

2. Experimental

Phosphorus-doped n-type Cz and Fz silicon wafers of (100) surface orientation were cut into 1×1 cm^2 sized samples. The doping concentration of the Cz and Fz wafers was $\sim 1.0 \times 10^{14}$ P cm^{-3} and $\sim 5.5 \times 10^{14}$ P cm^{-3}, respectively, and the oxygen content, as measured by secondary ion mass spectrometry (SIMS), was $\sim 2.7 \times 10^{17}$ cm^{-3} and below the SIMS detection limit of $\sim 3 \times 10^{16}$ cm^{-3}, respectively. The carbon concentration was below the SIMS detection limit of $\sim 5 \times 10^{15}$ cm^{-3} in both the Cz and Fz wafers. The samples were chemically cleaned using a standard procedure, including a final dip in diluted hydrofluoric acid [18]. 150 nm thick and circular palladium Schottky contacts (SC) were deposited using electron-beam evaporation and a shadow mask. Aluminum was thermally evaporated for back side Ohmic contacts with a thickness of 50 nm. The samples were mounted in a holder and the SC were wire bonded to the measurement terminals using 30 μm diameter gold wires minimizing shadowing during subsequent irradiation. The SC displayed a current rectification of ∼4 orders of magnitude between reverse and forward bias (−2 V and +2 V). The holder with the mounted samples was then loaded into a

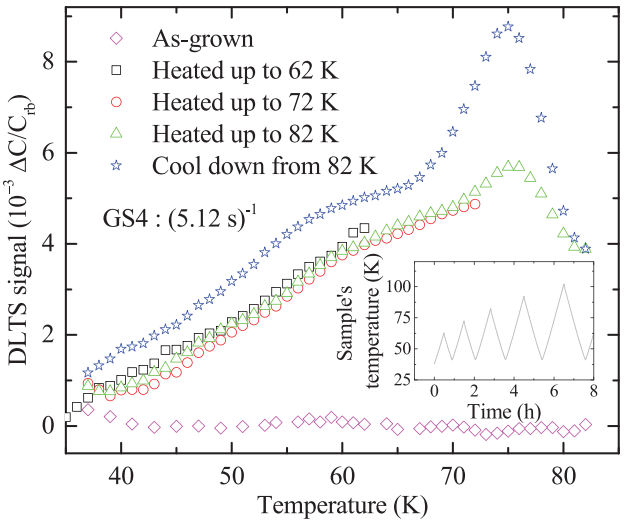

Figure 1. DLTS spectra of a *Cz* sample irradiated with $\sim 1 \times 10^{12}$ H^+ cm^{-2} at ∼30 K, Rate window = $(5.12\ s)^{-1}$. The inset shows the sample temperature versus time after irradiation. A GS4 weighting function was used to deduce the DLTS spectra from the recorded capacitance transients. For comparison, the spectrum of an as-grown sample before irradiation is also included.

closed-cycle helium cryostat (25–350 K) connected to one beam-line of the 1 MV NEC Tandem ion-accelerator in our laboratory. This was followed by cooling down with no SC bias applied and irradiation at the temperature of ∼30 K. The irradiation was performed with 2.0 MeV H^+ ions, having a projected range (R_p) of ∼45 μm, as estimated by Monte Carlo simulations using the SRIM code [19], and fluences ranging from $\sim 5 \times 10^{11}$ to $\sim 1.5 \times 10^{12}$ cm^{-2}. In order to reduce channeling, the samples were tilted by ∼5° with respect to the incident direction of the H^+ ion beam and further, the irradiations were performed through the 150 nm thick palladium contacts.

In one case, the irradiated sample was temperature cycled, i.e. heated and cooled down again to 30 K with increasing maximum temperature in stages of 10 K starting from ∼60 K. The temperature ramp rate was 1 K per min and concurrently, DLTS measurements were performed. In the other cases, the irradiated samples were heated with a rate of ∼5 K min^{-1} to a given temperature in the range of 70 K to 90 K and then isothermally annealed for durations up to 60 h while continuously recording the DLTS capacitance transients. The annealing temperatures were selected to coincide with the peak position of the $E_c - 0.17$ eV signal for a specific rate window and they were controlled with a resolution of 0.1 K. The DLTS spectra and the capacitance transients were acquired using the setup described in Ref. [20], applying a reverse bias of −15 V together with a filling pulse of 15 V and 50 ms duration. The rate windows employed were between $(20\ ms)^{-1}$ to $(12.8\ s)^{-1}$ with a weighting function of lock-in type or GS4 type [21].

3. Results and discussion

Figure 1 shows selected DLTS spectra of the sample undergone sequential heating and cooling cycles with increasing maximum temperature, as depicted in the inset. A GS4 weighting function was applied to enhance the energy resolution, and a rather broad shoulder with the indication of a peak at ∼60 K appears already during the first heating scan. In the subsequent scans to higher temperatures, the shoulder peak stays constant and does not evolve. This suggests strongly that the peak is due to either an intrinsic defect formed directly during the irradiation or a defect arising from trapping of *I*'s being mobile at 30 K. One possible candidate is the trivacancy center (V_3) which in its four-fold coordinated configuration (FCC) gives rise to a shallow acceptor level at $\sim E_c - 0.075$ eV [22], consistent with the position of the shoulder peak. This suggestion is also corroborated by the low generation rate of the peak, being about a factor of 50 lower than that of V^{2-} in the *Cz* samples (∼0.3 versus 15 cm^{-1}) where the latter value will be further discussed later. Figure 1 reveals also a distinct signal peaking at 75 K which grows in amplitude with increasing cycling temperature above 72 K; the peak is positioned at $\sim E_c - 0.17$ eV and assigned to the prominent *V*O center [15, 16]. A substantial increase in [*V*O] occurs for the cooling-down scan after reaching 82 K, evidencing the presence of mobile *V*'s and a diffusion length on the order of 20 nm during the 14 min of scanning from 75 to 82 K and back to 75 K.

No decreasing DLTS peak concurrent with the growth of [*V*O] is found and this holds at least for temperatures up 85 K using the rate window of $(5.12\ s)^{-1}$, figure 1. This indicates that the $V^{-/2-}$ level is located deeper than ∼0.19 eV below E_c, assuming an electron capture cross section of $\sim 10^{-15}$ cm^2 which is a typical value for acceptor states due to vacancy-type defects in silicon [23]. Similar results were obtained previously by Troxell and Watkins [13] and imply that the $V^{-/2-}$ level remains filled in the space charge region during the quiescent reverse bias stage of the DLTS measurements. With no reverse bias applied and temperatures below 90 K, the Fermi level is positioned at ∼0.07–0.08 eV below E_c in the probed volume of the studied samples.

Results for the growth of [*V*O] in the *Fz* and *Cz* samples after isothermal annealing at different temperatures are displayed in figures 2(a) and (b), respectively. The inset of figure 2(a) shows DLTS spectra of the *V*O level for different rate windows and illustrates how the annealing temperatures were selected, e.g. for annealing at 75.7 K a rate window of $(3.2\ s)^{-1}$ was used to continuously monitor the *V*O evolution. The growth in [*V*O] obeys first-order kinetics and can be described by

$$[VO] = [VO]_{sat}\,(1 - e^{-c(T)t}), \qquad (1)$$

where $[VO]_{sat}$ is the saturated concentration approached as the annealing duration becomes long, $c(T)$ is the temperature dependent rate constant and T is the absolute temperature. In accordance with equation (1), the experimental data in figures 2(a) and (b) are depicted as $\ln(1 - [VO]/[VO]_{sat})$ versus t and they exhibit a linear dependence where the slope is given by $c(T)$. First-order kinetics is, indeed, anticipated for the reaction $V + O_i \rightarrow VO$ since the irradiation-induced concentration of V is in the $10^{12} - 10^{13}$ cm^{-3} range whilst $[O_i]$ is in the 10^{17} cm^{-3} range for the *Cz* samples and expectedly in the 10^{15} cm^{-3} range for the *Fz* samples, i.e. $[O_i] \gg [V]$

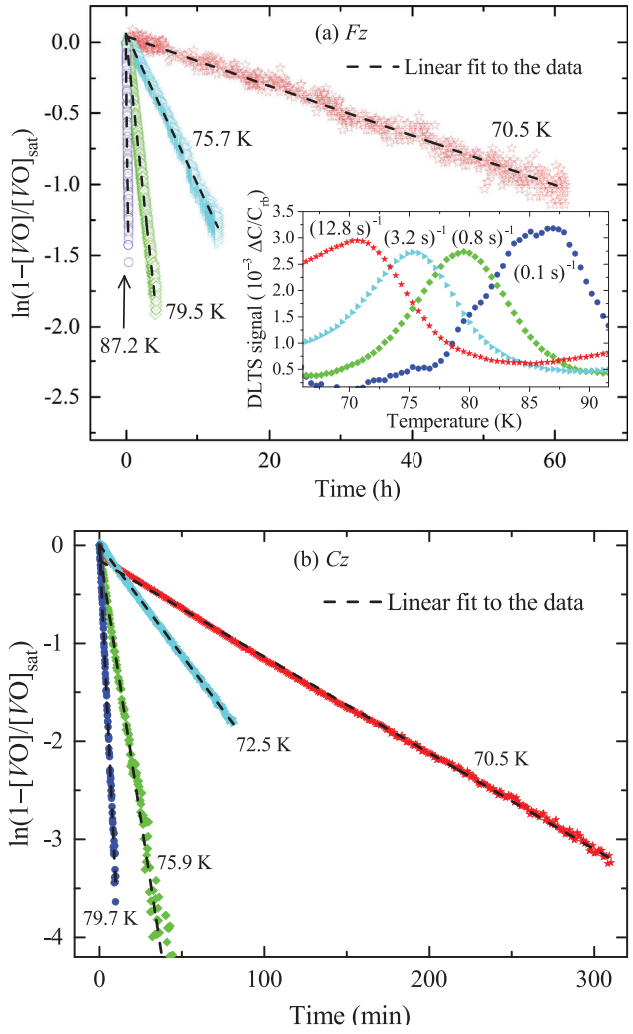

Figure 2. (a) $\ln(1-[VO]/[VO]_{sat})$ versus annealing time at 70.5, 75.7, 79.5 and 87.2 K for *Fz* samples irradiated with $\sim 1 \times 10^{12}$ H^+ cm^{-2} at ~30 K. The inset shows the DLTS spectra of the *VO* level using four different rate windows. (b) $\ln(1-[VO]/[VO]_{sat})$ versus annealing time at 70.5, 72.5, 75.9 and 79.7 K for *Cz* samples irradiated with $\sim 5 \times 10^{11}$ H^+ cm^{-2} at ~30 K. The dotted lines represent least-squares linear fits to the experimental data.

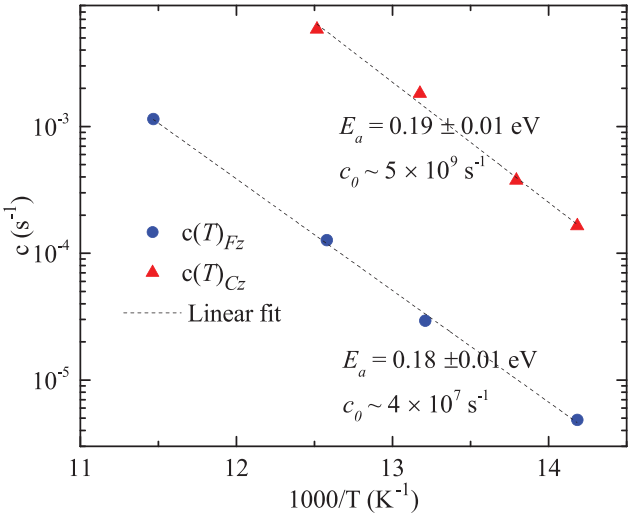

Figure 3. Arrhenius plot of the reaction rate values deduced versus 1000/*T*. The dotted lines represent linear fits of the reaction rates and the values extracted for the activation energy and pre-exponential factor of *c* are indicated.

in both cases. Moreover, the growth rate of [*VO*] is about a factor of 50 higher in the *Cz* samples compared to the *Fz* ones, reflecting $[O_i]_{Cz} \gg [O_i]_{Fz}$. The $c(T)$ values deduced by least-squares linear fitting of the data in figures 2(a) and (b) are shown versus 1000/*T* in figure 3. Both sets of results exhibit an activation energy, E_a, of ~0.18–0.19 eV which is attributed to the migration of V^{2-}. This value is identical with that found by Watkins [2] in an EPR study of counter-doped *n*-type *Cz* samples with a net carrier concentration of $\sim 3 \times 10^{16}$ cm^{-3} and subjected to MeV electron fluences of $\geqslant 10^{17}$ cm^{-2}. Hence, in the present study both the net doping concentration and the [*V*] are more dilute by about two orders of magnitude relative to those in [2], corroborating that the (0.18–0.19) eV value represents the activation energy for migration of V^{2-} over long distances.

As revealed by figure 3, the difference in the reaction rate $c(T)$ between the *Cz* and *Fz* samples arises from the pre-exponential factor, c_0. The c_0 values in figure 3 differ by about two orders of magnitude between the two sets of samples but the uncertainty is substantial since the extraction requires extrapolation of the linear curves to *T* equals infinity. In an attempt of a more accurate determination of the $c_0(Cz)/c_0(Fz)$ ratio, the $c(T)$ values obtained for the *Cz* and *Fz* samples annealed at the same temperatures within the experimental accuracy of ±0.1 K are directly compared, yielding $c_0(Cz) \approx 45\, c_0(Fz)$ as shown in figure 4. This gives $[O_i]_{Fz} \approx [O_i]_{Cz}/45 = 6 \times 10^{15}$ cm^{-3}, which appears as a reasonably estimate consistent with $[O_i]_{Fz}$ being below the SIMS detection limit ($\sim 3 \times 10^{16}$ cm^{-3}). Moreover, both the *Cz* and *Fz* data can now be used for deduction of the V^{2-} diffusivity ($D^{V^{2-}}$).

Applying the theory for diffusion-limited reactions [24, 25], one arrives at the following expression for the trapping rate of V^{2-} by O_i:

$$c(T) = 4\pi R[O_i]D^{V^{2-}} = 4\pi R[O_i]D_0^{V^{2-}} e^{-\frac{E_{migr}}{kT}}. \qquad (2)$$

Equation (2) assumes a capture radius *R* for the trapping process and O_i to be immobile [26]. Further, E_{migr} is the activation energy for migration of V^{2-} and *k* is Boltzmann's constant. In accordance with equation (2), $D^{V^{2-}}$ is obtained by dividing the experimental $c(T)$ values with $4\pi R[O_i]$, and the resulting Arrhenius plot is shown in figure 5. *R* is put equal to 10 Å governed by the defect geometry since no Coulomb force is expected to be present between the electrically inactive (neutral) O_i atom and V^{2-}. Taking all the $D^{V^{2-}}$ values into account for both the *Cz* and *Fz* samples covering a dynamic range of more than two orders of magnitude, E_{migr} becomes ~0.18 eV with $D_0^{V^{2-}} \approx 4 \times 10^{-3}$ cm^2 s^{-1}. The $D_0^{V^{2-}}$ value is identical to that predicted for a simple jump process in a cubic diamond lattice structure with the lattice parameter of silicon [27]. That is, no evidence of entropy effects is found for the migration of V^{2-}.

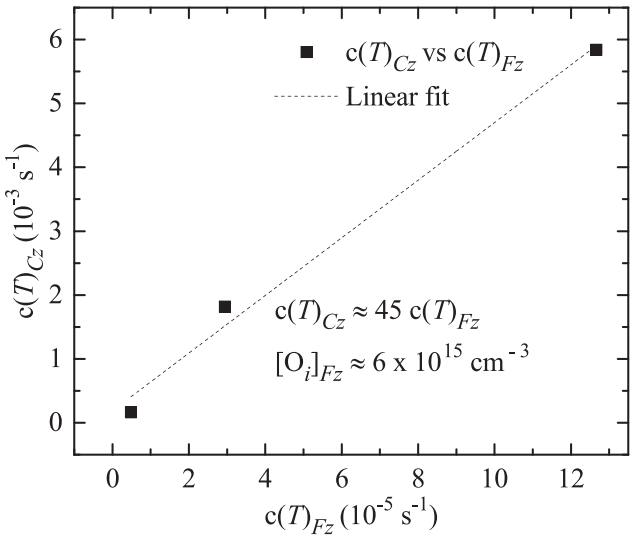

Figure 4. The reaction rate $c(T)$ in three Cz samples plotted against of that in three Fz samples, annealed at the same temperatures within the experimental accuracy (70.5 ± 0.1, 75.8 ± 0.1 and 79.6 ± 0.1 K).

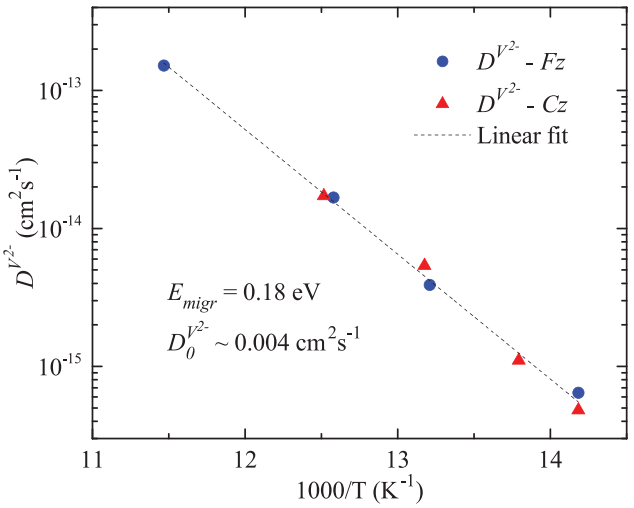

Figure 5. Arrhenius plot of the diffusivity of V^{2-} in the Fz and Cz samples, extracted from the corresponding c-values, versus 1000/T. The dotted line represents least-squares linear fit to the data points.

Finally, the absolute net generation rate of V's, as deduced from $[VO]_{sat}$ in the different samples, corresponds to a survival fraction on the order of ∼1% with regard to dynamic annealing. The ballistic generation rate is estimated to be ∼2000 V cm^{-1} from SRIM [19] simulations assuming a threshold energy of 20 eV for the displacement of Si atoms [28, 29] and considering the depth interval probed by the DLTS measurements ∼(2–10) μm. The fraction of ∼1% is of the same order of magnitude as that obtained for irradiation/implantation at RT [30] and implies that thermal processes activated in the 60 to 300 K range play no substantial role for the self-annihilation of V's and I's. In this context, it should also be underlined that the displacement of the Si atoms is anisotropic with the ⟨1 1 1⟩ direction being the easiest one for displacement [28, 31–34]. The 20 eV value refers to this direction but the recoiling Si atoms generated by collisions with the impinging H^+ ions will be distributed over a variety of directions. For most of these directions, the imparted energy required for atomic displacement will be larger than 20 eV, and the effective mean displacement energy may be two to three times larger than 20 eV. In a first approximation, the concentration of displaced Si atoms is inversely proportional to the displacement energy threshold [35, 36], and hence, the effective survival fraction may approach ∼3%.

4. Summary and conclusion

The double negatively charged mono-vacancy in silicon is found to be mobile at temperatures exceeding ∼70 K in lightly-doped n-type Cz and Fz samples containing a dilute concentration of irradiation-induced V's. O_i is a main residual impurity in the samples and a prevailing trap of the migrating V^{2-}. The transformation of V^{2-} to VO exhibits first-order kinetics and the rate is limited by the diffusivity of V^{2-} times $[O_i]$. A value of ∼0.18 eV is determined for the activation energy of V^{2-} migration, identical to that reported previously in the literature by other authors using EPR measurements and counter-doped Cz samples of medium resistivity. The pre-exponential factor deduced for the V^{2-} diffusivity is $\sim 4 \times 10^{-3}$ cm^2 s^{-1} and implies a simple jump process without entropy effects.

The energy position of the $V^{-/2-}$ transition level is deeper than $\sim E_c - 0.19$ eV. Because of the high mobility of V^{2-} and the high trapping rate at residual O_i atoms, the $V^{-/2-}$ level is elusive to DLTS measurements where charge carrier emission occurs via thermal excitation. In addition, the net generation rate of V is low even during irradiation at cryogenic sample temperatures, and the effective fraction of irradiation-induced V's surviving dynamic annealing is only on the order of ∼3% in the lightly doped n-type samples studied.

Acknowledgments

This work was supported by the University of Oslo and the Research Council of Norway through the Norwegian Micro- and Nano-Fabrication Facility, NorFab (197411/V30), which enabled the use of UiO MiNaLab and SINTEF MiNaLab.

References

[1] Watkins G D 1964 *Radiation Damage in Semiconductor* (Paris: Dunod) p 97
[2] Watkins G D 1974 Lattice defects in semiconductors *Institute of Physics Conf. (London, 1975)* vol 23 p 1
[3] Watkins G D, Troxell J R and Chatterjee A P 1978 Defects and radiation effects in semiconductors *Institute of Physics Conf. (London, 1979)* vol 46 p 16
[4] Watkins G D 1986 Chapter: the lattice vacancy in silicon *Deep Centers in Semiconductors* (New York: Gordon and Breach) p 178
[5] Watkins G D 1999 Chapter: intrinsic point defects in semiconductor *Handbook of Semiconductor Technology* vol 1 (New York: Wiley) p 121
[6] Watkins G D 2000 *Mater. Sci. Semicond. Process.* **3** 227–35

[7] Lannoo M, Baraff G A and Schlüter M 1981 *Phys. Rev.* B **24** 943
[8] Lannoo M 1983 *Phys. Rev.* B **28** 2403
[9] Hubbard J 1958 *Proc. R. Soc. A* **243** 336–52
[10] Baraff G A, Kane E O and Schlüter M 1979 *Phys. Rev. Lett.* **43** 956
[11] Watkins G D and Troxell J R 1980 *Phys. Rev. Lett.* **44** 593
[12] Newton J L, Chatterjee A P, Harris R D and Watkins G D 1983 *Physica* B + C **116** 219–23
[13] Troxell J R and Watkins G D 1980 *Phys. Rev.* B **22** 921
[14] Bemski G 1959 *J. Appl. Phys.* **30** 1195–8
[15] Watkins G D, Corbett J W and Walker R M 1959 *J. Appl. Phys.* **30** 1198–203
[16] Watkins G D and Corbett J W 1961 *Phys. Rev.* **121** 1001
[17] Corbett J W, Watkins G D, Chrenko R M and McDonald R S 1961 *Phys. Rev.* **121** 1015
[18] Taubenblatt M A, Thomson D and Helms C R 1984 *Appl. Phys. Lett.* **44** 895–7
[19] Ziegler J F, Ziegler M D and Biersack J P 2010 *Nucl. Instrum. Methods Phys. Res.* B **268** 1818–23
[20] Bhoodoo C, Hupfer A, Vines L, Monakhov E V and Svensson B G 2016 *Phys. Rev.* B **94** 205204
[21] Istratov A A 1997 *J. Appl. Phys.* **82** 2965–8
[22] Markevich V P, Peaker A R, Lastovskii S B, Murin L I, Coutinho J, Torres V J B, Briddon P R, Dobaczewski L, Monakhov E V and Svensson B G 2009 *Phys. Rev.* B **80** 235207
[23] Sah C T, Forbes L, Rosier L L and Tasch A F 1970 *Solid-State Electron.* **13** 759–88
[24] Waite T R 1957 *Phys. Rev.* **107** 463–70
[25] Waite T R 1958 *J. Chem. Phys.* **28** 103–6
[26] Stavola M, Patel J R, Kimerling L C and Freeland P E 1983 *Appl. Phys. Lett.* **42** 73–5
[27] Philibert J 1991 *Atom Movements: Diffusion and Mass Transport in Solids* (Les Ulis: Les Editions de Physique)
[28] Corbett J W and Watkins G D 1965 *Phys. Rev.* **138** A555
[29] Svensson B G and Lindström J L 1992 *J. Appl. Phys.* **72** 5616–21
[30] Svensson B G, Jagadish C, Hallén A and Lalita J 1997 *Phys. Rev.* B **55** 10498–507
[31] Haddad I N and Banbury P C 1966 *Phil. Mag.* **14** 829–40
[32] Banbury P C and Haddad I N 1966 *Phil. Mag.* **14** 841–6
[33] Hemment P L F and Stevens P R C 1969 *J. Appl. Phys.* **40** 4893–901
[34] Miller L A, Brice D K, Prinja A K and Picraux S T 1994 *Phys. Rev.* B **49** 16953–64
[35] Kinchin G H and Pease R S 1955 *Rep. Prog. Phys.* **18** 1–51
[36] Sigmund P 1969 *Phys. Rev.* **184** 383–416